

RF vs. Acceleration Power Distribution in Helicon Electrostatic Thruster

IEPC-2017-194

*Presented at the 35th International Electric Propulsion Conference
Georgia Institute of Technology • Atlanta, Georgia • USA
October 8 – 12, 2017*

Daisuke Ichihara¹, Yoshiya Nakagawa², Akira Iwakawa³ and Akihiro Sasoh⁴
Nagoya University, Nagoya, Aichi, 464-8603, Japan

Takuya Yamazaki⁵
Mitsubishi Heavy Industries, LTD, Nagoya, Aichi, 455-8515, Japan

Abstract: The effects of a radio-frequency (RF) power on the ion generation and electrostatic acceleration in helicon electrostatic thruster were investigated. A RF power that was even smaller than a direct-current (DC) power enhanced the ionization of the propellant, thereby both the ion beam current and energy were increased. However, an excessively large amount of RF power resulted in their saturation and consumed for generating doubly-charged ions. From the tradeoff between the ion production by the RF power and the electrostatic acceleration made by the DC discharge power, the thrust efficiency has a maximum value at an optimal RF to DC discharge power ratio of 1.0.

Nomenclature

e	= elementary charge
E_i	= ion beam energy
F	= thrust
\hat{J}_1	= propellant flow rate through the helicon plasma source in current equivalent
\hat{J}_2	= propellant flow rate through the hollow cathode in current equivalent
J_d	= discharge current
J_i	= total ion beam current
J_k	= keeper current
m_i	= ion mass
P_s	= RF power to the helicon plasma source
V_d	= discharge voltage
V_k	= keeper voltage
η	= thrust efficiency
θ	= half-beam divergence angle

I. Introduction

Owning to the high specific impulse capability, electric propulsion has an advantage over chemical propulsion. Based on the space propulsion principle, thrust and specific impulse have opposite dependence on the propellant

¹ Research associate, Department of Aerospace Engineering, ichihara@fuji.nuae.nagoya-u.ac.jp.

² Student, Department of Aerospace Engineering, nakagawa@fuji.nuae.nagoya-u.ac.jp.

³ Lecturer, Department of Aerospace Engineering, iwakawa@nuae.nagoya-u.ac.jp.

⁴ Professor, Department of Aerospace Engineering, sasoh@nuae.nagoya-u.ac.jp.

⁵ Deputy Manager, Electronics System Engineering Department

mass flow rate with a constant power¹. This competing performance of specific impulse and thrust should offset each other in the trade-off between payload ratio and working period. Because of its low thrust density, the working period becomes at least a hundred times longer than with chemical propulsion. A promising method to increase the thrust density is to utilize a helicon plasma source, which is capable of producing high-density plasma on the order of 10^{19} m^{-3} ². Harada et al³. demonstrated the electrostatic ion acceleration in a helicon electrostatic thruster (HEST); generated ions in the helicon plasma source by radio-frequency (RF) discharge were electrostatically accelerated by direct-current (DC) discharge. In ref **, we reported anode geometry effects on the ion acceleration characteristics of HEST. In this paper, the RF power effects on the ion acceleration characteristics were studied in order to quantitatively investigate the power matching between RF plasma generation and electrostatic acceleration in HEST.

II. Experimental apparatus

Figure 1 shows a schematic of the HEST. HEST has a RF plasma source in the upstream region and electrostatic acceleration electrodes in the downstream region. The RF plasma source was comprised of a ceramic (Photoveel) tube with an inner diameter of 27 mm and length of 150 mm. The exit of the RF plasma source was located at the center of the solenoid coil. The magnetic field strength was 100 mT at the coil center. A copper ring anode with an inner diameter of 27 mm and thickness of 10 mm was placed 25 mm axially downstream from the coil center. In the downstream region, the magnetic field was greatly modified using 16 cylindrical Nd-Fe-B permanent magnets and soft iron yokes to generate a diverging magnetic field followed by a field-free region where the magnetic field strength was less than 3 mT. A commercial hollow cathode (DLHC-1000, Kaufman & Robinson Inc.) was used and its orifice was placed 70 mm off-axis at 175 mm axially downstream from the coil center. The RF power frequency was set to 13.56 MHz. Argon gas (99.9999% of purity) was supplied for both the helicon plasma source and the hollow cathode.

To evaluate the ion beam energy E_i from an ion energy distribution function (IEDF), a retarding potential analyzer (RPA) was used. The ion beam current J_i and half-beam divergence angle $\langle\theta\rangle$ were measured using a nude Faraday probe. In order to measure the beam currents of singly and doubly charged ions, an $E \times B$ probe was used. The detailed designs and data procedures of RPA, nude Faraday cup, and $E \times B$ probe were reported in our previous works³⁻⁵.

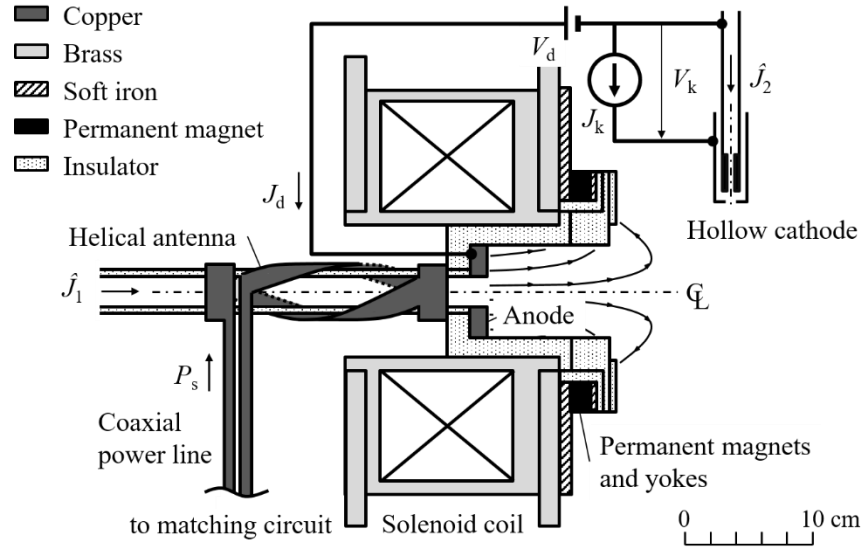


Figure 1. Schematic and electrical circuit of HEST.

III. Experimental results

A. Operating conditions

All experiments were conducted in a 3.2-m-long and 1.2-m-diameter, stainless steel vacuum chamber. The ambient pressure in the vacuum chamber, measured by an ionization gauge, was maintained lower than 10 mPa with a total working gas flow rate of 1.36 Aeq. The working gas flow rate supplied to the plasma source \hat{J}_1 was set to 0.5 or 1.0 Aeq, and the RF power to the plasma source P_s was increased from 0 to 1500 W. The discharge voltage V_d was set to

300 V. The hollow cathode was operated with a working gas flow rate, \hat{J}_2 , of 0.36 Aeq, and the keeper current J_k was set to 2.0 A. Each operation condition for measuring E_i , J_i , $\langle\theta\rangle$, J_d , and keeper voltage V_k was repeated at least twice. The operation time was at least 3.5 s at each operating condition.

B. Operating characteristics

Table 1 summarizes the operation characteristics as varying P_s in $\hat{J}_1 = 0.5$ Aeq case. J_i increased with P_s . In particular, J_i increased from 0.07 to 0.46 as P_s increased from 0 to 100 W. When $P_s > 100$ W, J_i increased more gradually. At $P_s = 1500$ W, J_i was equal to 0.80 A, which is 93% of the total supplied flow rate $\hat{J}_1 + \hat{J}_2$. Same as J_i , E_i increased quickly as increasing P_s from 0 to 100 W. At $P_s = 1500$ W, E_i reached 265 eV, which is 88% of V_d . Therefore, the RF plasma source contributed to both the ion generation and electrostatic acceleration.

Table 1. Operation characteristics with $\hat{J}_1=0.5\text{Aeq}$, $\hat{J}_2=0.36\text{Aeq}$, $V_d=300\text{V}$.

P_s , W	J_i , A	E_i , eV	$P_s/(J_d V_d)$	η , %
0	0.07	133	0	0.4
100	0.46	197	0.34	5.1
200	0.56	213	0.59	6.3
300	0.61	224	0.81	6.6
400	0.64	232	1.03	6.6
500	0.67	235	1.25	6.5
1000	0.73	252	2.30	5.4
1500	0.80	265	3.32	4.8

Table 2 summarizes the operation characteristics as varying P_s in $\hat{J}_1 = 1.0$ Aeq case. In the $P_s = 0$ W operation, J_i was equal to 1.0 A, which is 77% of $\hat{J}_1 + \hat{J}_2$. In general, J_i increased with P_s . However, J_i had a local minimum at $P_s = 100$ W. When $P_s > 100$ W, J_i increased with P_s . At $P_s = 400$ W, J_i was equal to the value of $\hat{J}_1 + \hat{J}_2$, and, at $P_s = 1500$ W, J_i was 1.2 times larger than $\hat{J}_1 + \hat{J}_2$. According to the current fraction of each charge-state ion measured by the $E \times B$ probe, the doubly charged argon ion current had 22% of J_i at $P_s = 500$ W and increased to 27% at $P_s = 700$ W. E_i showed different trend from $\hat{J}_1 = 0.5$ Aeq case. E_i maintained approximately 60 eV and then increased from $P_s = 200$ W. However, E_i was gradually saturated at approximately 220 eV, which is 73% of V_d . From the $E \times B$ probe measurement in the $P_s = 600$ W operation, the effective acceleration voltage of a singly charged and doubly charged argon ion were 186 V and 143 V, respectively. This results indicate that, in this $\hat{J}_1 = 1.0$ Aeq operation, the contribution of P_s to the increase of E_i was limited because of the generation of low-energy doubly charged ions.

Table 2. Operation characteristics with $\hat{J}_1=1.0\text{Aeq}$, $\hat{J}_2=0.36\text{Aeq}$, $V_d=300\text{V}$.

P_s , W	J_i , A	E_i , eV	$P_s/(J_d V_d)$	η , %
0	1.06	63	0	2.7
100	0.83	59	0.23	2.2
200	1.00	63	0.39	2.7
300	1.27	99	0.43	4.9
400	1.35	149	0.47	7.0
500	1.41	175	0.53	8.0
1000	1.54	216	0.92	8.7
1500	1.65	223	1.34	8.4

C. Input power dependence of thrust performance

In this section, thrust performances such as thrust F and thrust efficiency η are estimated. Considering only singly charged ions, F and η are calculated as in Eqs. (1) and (2), respectively.

$$F = J_i \sqrt{\frac{2m_i E_i}{e}} \cos\langle\theta\rangle \quad (1)$$

$$\eta = \frac{F^2}{2m_i (\hat{J}_1 + \hat{J}_2) / e \cdot (P_s + J_d V_d + J_k V_k)} \quad (2)$$

Here, m_i and e are ion mass and elementary charge, respectively. Table 1 and 2 also summarize $P_s/(J_d V_d)$, which is the RF power ratio against the electrostatic acceleration power, and calculated η . By varying $P_s/(J_d V_d)$, η achieved a peak value of 6.6% and 8.7% at $P_s/(J_d V_d) \approx 1.0$ in $J_1 = 0.5$ Aeq and 1.0 Aeq case, respectively. In $P_s/(J_d V_d) < 1.0$, increasing P_s contributed ion generation in the helicon plasma source and J_i increased rapidly. Therefore, both F and η increased. However, inputting large amount of P_s was enhanced generating doubly charged ions and contribution for ion acceleration was limited. As a result, η decreased in $P_s/(J_d V_d) > 1.0$ operation.

IV. Conclusions

In this paper, the effects of RF power for the plasma source on the ion generation and its electrostatic acceleration were evaluated. By inputting small of RF power, ion generation were enhanced in the plasma source. However, inputting large amount of RF power caused generating doubly charged ions. The thrust efficiency was governed by the RF power ratio against to electrostatic acceleration power. The thrust efficiency reached maximum value at the RF power ratio against to electrostatic acceleration power of about 1.0.

Acknowledgments

This work was supported by JSPS KAKENHI (JP15H02321) and by Mitsubishi Heavy Industries Ltd.

References

- ¹ G. P. Sutton and O. Biblarz, *Rocket Propulsion Elements*, 7th ed., John Wiley & Sons, Inc., New York, 2001, Chaps. 2, 36.
- ² C. Charles, "Plasmas for spacecraft propulsion," *Journal of Physics D: Applied Physics*, Vol. 42, 163001, 2009.
- ³ S. Harada, T. Baba, A. Uchigashima, S. Yokota, A. Iwakawa, A. Sasoh, T. Yamazaki, and H. Shimizu, "Electrostatic acceleration of helicon plasma using a cusped magnetic field," *Applied Physics Letters*, Vol. 105, 194101, 2014.
- ⁴ Akira Uchigashima, Teruaki Baba, Daisuke Ichihara, Akira Iwakawa, Akihiro Sasoh, Takuya Yamazaki, Shota Harada, Matsutaka Sasahara and Tomoji Iwasaki, "Anode Geometry Effects on Ion Beam Energy Performance in Helicon Electrostatic Thruster," *IEEE Transactions on Plasma Science*, Vol. 44, No. 3, 2016, pp. 306-313.
- ⁵ D. Ichihara, Y. Nakagawa, A. Uchigashima, A. Iwakawa, A. Sasoh, and T. Yamazaki, "Power matching between plasma generation and electrostatic acceleration in helicon electrostatic thruster," *Acta Astronautica*, Vol. 139, 2017, pp. 157-164.